

# On the renormalization of contact interactions for the configuration-interaction method in two dimensions

Massimo Rontani<sup>1</sup>, G Eriksson<sup>2</sup>, S Åberg<sup>2</sup> and S M Reimann<sup>2</sup>

E-mail: [massimo.rontani@nano.cnr.it](mailto:massimo.rontani@nano.cnr.it)

<sup>1</sup> CNR-NANO, Via Campi 213a, 41125 Modena, Italy

<sup>2</sup> Mathematical Physics, LTH, Lund University, P. O. Box 118, 22100 Lund, Sweden

**Abstract.** The configuration interaction (CI) method for calculating the exact eigenstates of a quantum-mechanical few-body system is problematic when applied to particles interacting through contact forces. In dimensions higher than one the approach fails due to the pathology of the Dirac  $\delta$ -potential, making it impossible to reach convergence by gradually increasing the size of the Hilbert space. However, this problem may be cured in a rather simple manner by renormalizing the strength of the contact potential when diagonalizing in a truncated Hilbert space. One hereby relies on the comparison of the CI results to the two-body ground-state energy obtained by the exact solution of the Schrödinger equation for a regularized contact interaction. We here discuss a scheme that provides cutoff-independent few-body physical observables. The method is applied to a few-body system of ultracold atoms confined by a two-dimensional harmonic oscillator.

PACS numbers: 67.85.-d, 31.15.ac, 67.85.Lm, 03.75.Ss

Submitted to: *J. Phys. B: At. Mol. Phys.*

## 1. Introduction

Trapped ultracold atom gases [1–7] are an ideal laboratory for the investigation of many-body physical phenomena. From a theoretical perspective, a major issue is the complexity of the atom-atom interaction potential which in numerical simulations can hardly be considered in its full form. However, one often is only interested in the low-energy scattering properties which in many cases may be accounted for by simple pseudopotentials. A standard approximation to model the atom-atom interactions in an ultracold gas of fermionic or bosonic atoms is a contact potential [8] describing the  $s$ -wave isotropic scattering by means of only one parameter, the scattering length  $a$ . For cold atom gases this pseudopotential has been widely and successfully used (see for example references [1–7]). However, the use of such pointlike interactions is mathematically troublesome [8]. In their simple form of Dirac  $\delta$ -functions contact potentials are unphysical in two and three dimensions and one needs to introduce a proper regularization [9–21]. In addition, there are subtle drawbacks which become particularly relevant when trying to solve the many-particle problem exactly. The crux of the matter (as noted by Huang [8]) lies in the fact that the regularized operators may be non-Hermitian, which prohibits finding their eigenvalues by variational methods. In particular, the direct diagonalization of the Hamiltonian on a *complete* space cannot be applied [8, 17, 22], unless the class of allowed basis wave functions obeys special (and often impractical) boundary conditions [19]. This also invalidates the direct application of the contact potential in the so-called configuration interaction (CI) approach ‡ (also known as the method of ‘exact diagonalization’). In the limit of small particle numbers and not too strong interactions the CI approach would otherwise allow an accurate treatment of correlation effects, also giving access to excited states [28–33]. It is therefore desirable to develop a scheme that can incorporate the regularization in a simple and straightforward manner.

In this paper we discuss a renormalization procedure for few-body systems with contact interactions in two dimensions (2D). For the confinement we choose the example of a 2D harmonic oscillator, a system that has been widely investigated in the context of ultracold atomic gases [34] and whose exact two-body states are known [17]. From a computational point of view, the 2D case is simpler than the three-dimensional one, however providing a similar complexity of the problem at hand. The renormalization procedure that we discuss here is similar in spirit to the ultraviolet renormalization adopted in analogous contexts by means of diverse techniques, including space discretization [35, 36], dimensional [14] and momentum-cutoff regularization [14, 19, 37–46], and other approaches [47–51]. We demonstrate explicitly how in a truncated Hilbert subspace with properly renormalized interactions the CI algorithm correctly reproduces the exact energies and wave functions of both ground and excited states, except when the relative distance between the particles becomes too small. The coupling constant of the contact potential employed in the calculation can be mapped onto the two-dimensional scattering length  $a$ . However, this mapping significantly depends on the energy cutoff. A relation between these quantities is established for the case of two particles confined in a 2D harmonic trap, for which the exact regularized solutions are available [17]. For three particles, the method is further validated through a comparison of semi-analytical results [52] with the CI data. The procedure can then also be applied in the case of larger systems, where such

‡ Other model interactions have been considered in the CI literature, such as Gaussian [23–27] and Morse [19] potentials.

analytic solutions do not exist. As a case study for the latter, we further compute the low-lying energy spectrum of  $N$  fermions confined in a harmonic trap, with  $N \leq 5$ . The CI results suggest that when diagonalizing in a truncated Hilbert space, by adapting the coupling constant one can accurately evaluate cutoff-independent  $N$ -body physical observables.

## 2. The two-body problem treated in relative coordinates

In order to investigate the nature of the contact interactions let us begin with the simple case of two interacting particles in a two-dimensional harmonic trap of frequency  $\omega_0$ . Throughout this paper we use as energy unit  $\hbar\omega_0$  and as length unit the oscillator length,  $\ell_0 = (\hbar/m\omega_0)^{1/2}$ . The two-body Hamiltonian, conveniently written in the center-of-mass and relative-motion coordinates  $\mathbf{R} = (\mathbf{r}_1 + \mathbf{r}_2)/2$  and  $\mathbf{r} = \mathbf{r}_1 - \mathbf{r}_2$ , respectively, then reads as

$$H_2 = H_{\text{com}} + H_{\text{rel}}, \quad (1)$$

with

$$H_{\text{com}} = -\frac{1}{4}\nabla_{\mathbf{R}}^2 + R^2 \quad (2)$$

and

$$H_{\text{rel}} = -\nabla_{\mathbf{r}}^2 + \frac{1}{4}r^2 + g\delta(\mathbf{r}) \quad (3)$$

where  $g$  is the coupling constant in units of  $(\hbar\omega_0)\ell_0^2$ . While the center-of-mass eigenstates of  $H_{\text{com}}$  are simply (2D) harmonic oscillator orbitals in the  $\mathbf{R}$  coordinate with trivial integer energies  $E_{\text{com}}$ , the non-trivial part of the two-body Hamiltonian,  $H_{\text{rel}}$ , pertains to the relative motion. If the relative-motion angular momentum  $M_{\text{rel}}$  is even (odd), the solution equally holds for spinless bosons and spinful fermions with total spin zero (one). Here we investigate the low-lying singlet states of either two spinless bosons or two fermions of opposite spin 1/2.

Solving the eigenvalue problem for  $M_{\text{rel}} = 0$  one diagonalizes the matrix

$$\langle n' | H_{\text{rel}} | n \rangle = (2n + 1)\delta_{n,n'} + \frac{g}{2\pi}, \quad (4)$$

where  $|n\rangle = \varphi_n(\mathbf{r}) \equiv \varphi_{n0}(\mathbf{r})$  stands for the 2D oscillator orbital in the  $\mathbf{r}$ -space with  $n$  nodes in the radial direction and angular momentum  $m = 0$  (the other sectors with  $M_{\text{rel}} \neq 0$  are trivial since off-diagonal matrix elements are zero). The explicit orbital form is  $\varphi_n(r) = (2\pi)^{-1/2}L_n(r^2/2)e^{-r^2/4}$ , where  $L_n(z)$  is the Laguerre polynomial of order  $n$ . In practice, one must restrict the number of basis functions,  $N_b$ , with  $N_b = n_{\text{max}} + 1$  and  $n_{\text{max}}$  being the number of nodes of the highest-energy orbital. For any  $g < 0$ , the ground-state energy obtained from the direct diagonalization of the matrix (4) does not converge but decreases monotonously as the basis size  $N_b$  increases. For  $g > 0$ , however, the energy converges to the noninteracting value (i.e., unity) [16]. Such behavior could also be expected from the fact that the offdiagonal Hamiltonian matrix elements are independent from  $n$ , as shown by (4) §. This clearly shows the pathology of the contact interaction in dimensions higher than one.

§ Considering the limiting case of very large interaction strength  $|g|$ , the Hamiltonian can be approximately written in matrix form as  $H_{\text{rel}} \approx \mathbf{I} + g/(2\pi)\mathbf{1}$ , where  $\mathbf{I}$  is the identity and  $\mathbf{1}$  is the  $N_b \times N_b$  matrix with all elements equal to one. For large values of  $N_b$ , for  $g \gg 0$  the lowest eigenvalue is unity, i.e., the contact interaction does not provide any scattering. For  $g \ll 0$ , one obtains  $-|g|N_b/(2\pi)$ , i.e., the ground-state energy diverges with  $N_b$  for attractive interaction [16]. Note that in the well behaved one-dimensional case the off-diagonal element is either zero or it decreases with  $n$  as  $\sim (-1)^{(n+n')/2}(nn')^{-1/4}$ .

### 2.1. Exact solution

A proper solution of the two-body problem consists in introducing a regularized contact potential. This path was followed by Busch and coworkers [17], whose results we partly recall in this section. Olshanii and Pricoupenko [53] provided a general form of the pseudopotential,  $V_{\text{pseudo}}$ , which should replace the simple Dirac  $\delta$ -function in  $H_{\text{rel}}$ ,

$$V_{\text{pseudo}} = -\frac{2\pi\delta(\mathbf{r})}{\ln(\mathcal{A}a\Lambda)} \left[ 1 - \ln(\mathcal{A}\Lambda r) r \frac{\partial}{\partial r} \right]_{r \rightarrow 0^+}, \quad (5)$$

where  $\Lambda$  is an arbitrary constant,  $a$  is the two-dimensional scattering length,  $\mathcal{A} = e^\gamma/2$ , and  $\gamma = 0.5772\dots$  is the Euler-Mascheroni constant.

The eigenstates of the regularized form of the relative-motion Hamiltonian,  $H_{\text{rel}}^{\text{reg}}$ , with

$$H_{\text{rel}}^{\text{reg}} = -\nabla_{\mathbf{r}}^2 + \frac{1}{4}r^2 + V_{\text{pseudo}}, \quad (6)$$

are obtained by imposing that the wave functions,  $\Psi(\mathbf{r})$ , written as linear superpositions of the orbitals  $\varphi_n(\mathbf{r})$  with unknown coefficients  $c_n$ ,

$$\Psi(\mathbf{r}) = \sum_{n=0}^{\infty} c_n \varphi_n(\mathbf{r}), \quad (7)$$

must solve the eigenvalue problem

$$H_{\text{rel}}^{\text{reg}} \Psi(\mathbf{r}) = E_{\text{rel}}^{\text{reg}} \Psi(\mathbf{r}). \quad (8)$$

Equations (7) and (8), together with the requirement of normalization, determine both the coefficients  $c_n$  and the energy  $E_{\text{rel}}^{\text{reg}}$ , the latter through the equation

$$\psi(1/2 - E_{\text{rel}}^{\text{reg}}/2) = \ln(2/a^2), \quad (9)$$

where  $\psi(z)$  is the digamma function of argument  $z$  ||.

The total energy  $E^{\text{reg}} = E_{\text{rel}}^{\text{reg}} + E_{\text{com}}$  is plotted as a function of  $\ln(d/a)$  in figure 1, with  $d = \sqrt{2}$  being the harmonic oscillator length in the relative frame (the scattering length  $a$  is always positive in two dimensions, as discussed e.g. in Ref. [54]). The wave function is

$$\Psi(\mathbf{r}) \propto U(-\nu, 1, r^2/2) e^{-r^2/4}, \quad (10)$$

where  $\nu = (E_{\text{rel}}^{\text{reg}} - 1)/2$  and  $U(a, b, z)$  is the confluent hypergeometric function.

The key point in the derivation of (9) is that one is not allowed to interchange the limiting procedure contained in the definition (5) of  $V_{\text{pseudo}}$ ,  $\lim_{r \rightarrow 0^+} \partial/\partial r$ , with the infinite summation appearing in (7),  $\sum_{n=0}^{\infty}$ . In fact, by doing so, the ‘regularizing’ part of the pseudopotential,  $\lim_{r \rightarrow 0^+} \ln(\mathcal{A}\Lambda r) r \partial/\partial r$ , provides a null result when applied to each addendum  $\varphi_n(\mathbf{r})$  of the sum, which is well behaved at the origin. In this case, the only possible solution of (8) is the noninteracting one. For the same reason, the regularization of  $V_{\text{pseudo}}$  is useless if the expansion (7) is finite, as it is of course always the case when diagonalizing numerically, making the regularization procedure irrelevant in this case.

|| Equation (9) actually differs from (21) of reference [17] for a numerical factor which is due to the different definition of  $a$ . Our usage here is consistent with the pseudopotential definition (5).

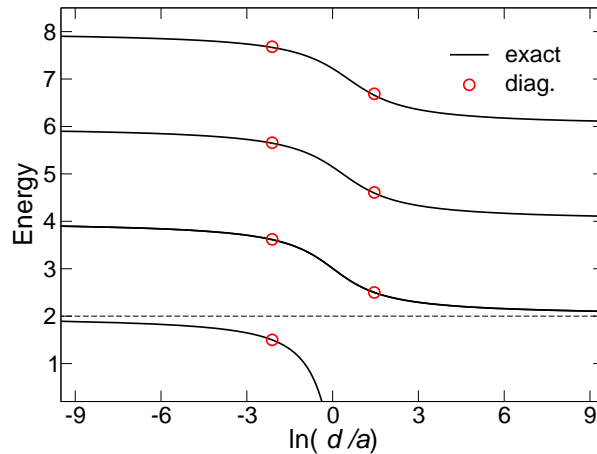


**Figure 1.** (color online). Exact energy spectrum  $E^{\text{reg}}$  of two particles (either fermions with total spin zero or spinless bosons) versus two-dimensional scattering length  $a$ . The circles show the energies obtained by direct diagonalization given in table 1 and the dashed line is the noninteracting ground-state energy.  $d = \sqrt{2}$  is the harmonic-oscillator length in the relative frame and  $M_{\text{rel}} = 0$ .

## 2.2. Diagonalization in a finite Hilbert space

Let us now investigate whether it is possible to perform a numerical diagonalization with the bare  $\delta$ -interaction in a truncated Hilbert space and to relate the result to the regularized solution. We here still restrict ourselves to the two-body case. The eigenvalues are obtained by performing the diagonalization in a given basis set, i.e., for a given value of  $N_b$ , at a fixed value of the coupling constant  $g$ . The result naturally depends on the number  $N_b$  of orbitals used. In order to obtain results which nevertheless can be interpreted physically we suggest to

- (i) Fix the Hilbert space size for the two-body system, i.e.,  $N_b$ .
- (ii) Link the value of the coupling constant  $g$  to be used in the direct diagonalization to the physically meaningful value of the exact, fully regularized two-body ground-state (GS) energy for a given scattering length  $a$ ,

$$\mathcal{E} \equiv E_{\text{GS}}^{\text{reg}}(a) = E_{\text{GS}}^{\text{diag}}(g, N_b). \quad (11)$$

Here  $E_{\text{GS}}^{\text{diag}}(g, N_b)$  is the energy obtained by the direct diagonalization for a specific value of  $g$  in a given basis set with fixed  $N_b$ , and  $E_{\text{GS}}^{\text{reg}}(a)$  is the desired regularized two-body ground-state energy that we in the following denote as  $\mathcal{E}$  (the value  $\mathcal{E} = 2$  is the energy in the noninteracting case,  $g = 0$ ).

In the following, we evaluate the above procedure by comparing the results obtained through direct diagonalization with the exact and fully regularized results that are available in the literature, i.e., energies and wave functions of two-body excited states [17] (Sec. 2.3) as well as exact eigenstates for three particles [52] (Secs. 3.1 and 3.2). This also allows to estimate the error associated with the truncation of the Hilbert space size.

**Table 1.** Comparison between exact regularized and directly diagonalized two-body energies for both ground and excited states, for attractive (2nd and 3rd column) and repulsive (4th and 5th column) interaction, respectively. The exact regularized ('exact') and the diagonalized ('diag.') data are linked by matching the corresponding GS energies, providing  $(a, g) = (11.71, -1.855)$  and  $(0.3294, 30.78)$  for  $\mathcal{E} = 1.500$  and  $2.500$ , respectively, where  $a$  is obtained by solving (9) and  $g$  is obtained by diagonalizing (4) with  $N_b = 13$ .

level	$g < 0$		$g > 0$	
	exact	diag.	exact	diag.
ground state	1.500	1.500	2.500	2.500
1st excited	3.613	3.619	4.596	4.608
2nd excited	5.647	5.657	6.658	6.688
3rd excited	7.666	7.680	8.706	8.757

### 2.3. Energies and wave functions of two-body excited states

For two particles described in relative coordinates, let us now fix the Hilbert space size through the number of relative orbitals  $N_b$  and consider two cases, corresponding to repulsive and attractive interaction, respectively. As a specific example, we set  $N_b = 13$ . Within this restricted space, we then chose as an example the two-body GS energies  $\mathcal{E} = 1.500$  and  $\mathcal{E} = 2.500$ . In the direct diagonalization of (4) these energies are obtained with the coupling constants  $g = -1.855$  and  $g = 30.78$ , respectively.

Note from figure 1 that  $\ln(d/a)$  assumes both positive and negative values, with the noninteracting ground-state energy (dashed line) being reached at both infinities on the real axis. Therefore, moving away from the  $\mathcal{E} = 2$  asymptotic value at  $\ln(d/a) = \pm\infty$  by increasing (decreasing) continuously the energy allows us to identify the branch that physically corresponds to repulsive (attractive) interaction, i.e.,  $g > 0$  ( $g < 0$ ). Solving (11) numerically for  $\mathcal{E} = 1.500$  and  $\mathcal{E} = 2.500$  we respectively obtain  $a = 11.71$  and  $a = 0.3294$  (cf. the two lowest-lying circles in figure 1).

Let us first compare the energies and wave functions of the two-body excited states obtained by direct diagonalization of (4) to the analogous exact and properly regularized quantities obtained from the knowledge of  $a$  through (9) and (10).

This is done in figure 1 and table 1 that compare energy levels up to the third excited state. For the chosen coupling strength  $g$ , the energies obtained by direct diagonalization (circles in figure 1) nicely match the regularized exact solution (solid lines), the worst relative error being only 7 parts per thousand (for the 3rd excited level in the repulsive case, cf. table 1) for our example of  $N_b = 13$ . This very good agreement is confirmed by the wave function analysis, reported in figures 2(a) and (b) for attractive and repulsive interaction, respectively.

The plots compare the radial probability densities of finding two particles at distance  $r$ , up to the third excited state. We see in both attractive and repulsive cases (figures 2(a) and (b), respectively) that the overlap of the probability densities as well as the agreement regarding node locations is almost perfect far from the origin, but becomes progressively worse as  $r \rightarrow 0$ . In fact, the square modulus of the exact regularized wave function presents a logarithmic singularity at the origin, originating from the behavior of the hypergeometric function of (10):

$$\Psi(r) \approx \frac{A}{\Gamma(-\nu)} [\ln r^2 + \psi(-\nu)] \quad \text{for } r \approx 0,$$

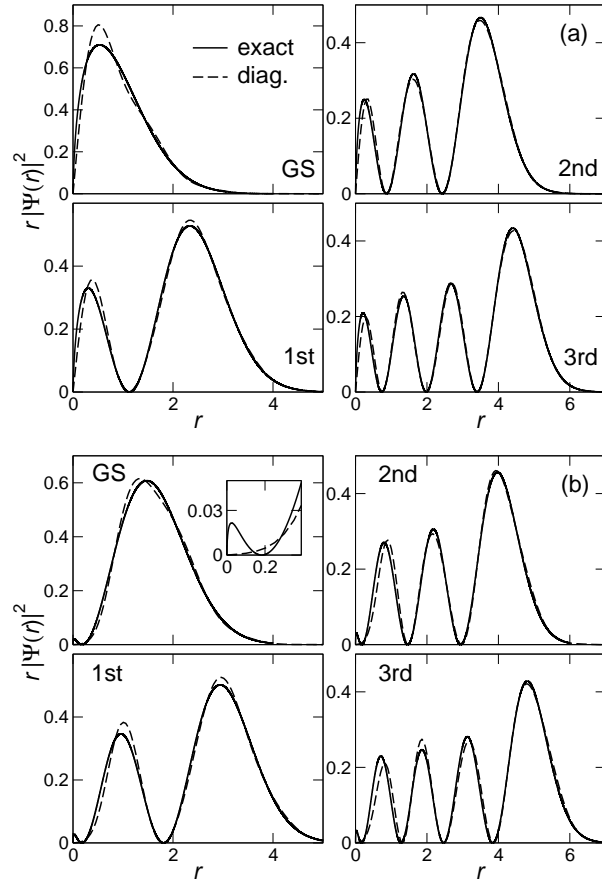


**Figure 2.** Radial probability density  $r|\Psi(r)|^2$  of finding two particles at distance  $r$ , from both the regularized exact solution (solid lines) and the direct diagonalization for fixed  $N_b$  and renormalized coupling constant  $g$  (dashed lines), for attractive (a) and repulsive (b) interaction, respectively. The panels display the ground (GS), first- (1st), second- (2nd), and third-excited (3rd) states. Here  $\Psi(r)$  is the relative-motion wave function normalized as  $\int dr r |\Psi(r)|^2 = 1$  for the exact regularized and the directly diagonalized solutions, respectively. The GS energy  $\mathcal{E}$  is 1.500 and 2.500 implying scattering lengths  $a = 11.71$  and 0.3294 for attractive (a) and repulsive (b) interaction, respectively, whereas the renormalized coupling constant used in the CI diagonalization is  $g = -1.855$  and 30.78, respectively, corresponding to a single-particle basis of  $N_b = 13$  orbitals. The energies of the states considered here are displayed in the 2nd and 3rd (4th and 5th) columns of table 1 for attractive and repulsive interaction, respectively, as well as in figure 1. The inset in the GS panel of figure (b) is a blow-up close to the origin.

where  $A$  is a normalization constant. Note the appearance of a node in the exact ground-state wave function for repulsive interaction [cf. inset of figure 2(b)], due to the occurrence of a strongly bound molecular state that is much deeper in energy ¶. Any expansion over a finite set of basis functions regular at the origin is unable to reproduce the logarithmic singularity. However, in 2D this is expected to have little effect on the calculations of observables dominated by the whole range of  $r$ .

#### 2.4. Truncation of the Hilbert space and short-distance cutoff

To understand the consequences on the wave function let us take a look at the evolution of the ground state obtained through direct diagonalization when the parameter  $N_b$  (controlling the energy cutoff in the single particle basis in relative coordinates [55,56]) is increased, going from dotted to dashed curves in figure 3, respectively. We see the same trend for both attractive (a) and repulsive (b) interactions, with the weight of  $r|\Psi_{\text{diag}}(r)|^2$  from the direct-diagonalization result shifting towards the origin. This increases the overlap with the regularized exact radial density  $r|\Psi_{\text{exact}}(r)|^2$ . This behavior suggests that the effect of the cutoff in the direct diagonalization is to provide a complementary short-distance cutoff  $r_c$  in real space, the larger  $N_b$  (higher energy cut-off) the smaller  $r_c$  (better resolution).

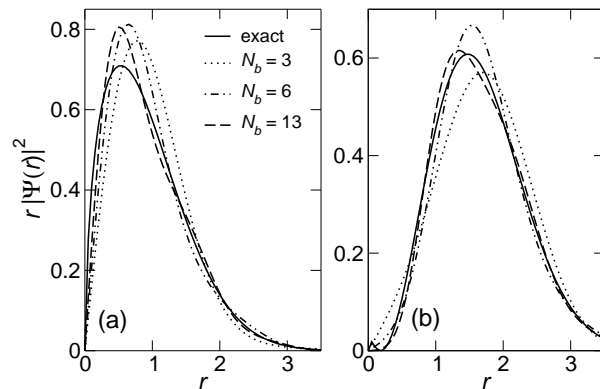


**Figure 3.** Radial probability density  $r|\Psi(r)|^2$  of finding two particles at distance  $r$  obtained from the direct diagonalization of (4) over subspaces of increasing  $N_b$ . Here  $\Psi(r)$  is the relative-motion wave function normalized as  $\int dr r|\Psi(r)|^2 = 1$ . The solid lines are the data from the regularized exact solution corresponding to  $a = 11.71$  and  $0.3294$  for attractive (a) and repulsive (b) interaction, respectively. The values of the coupling constants  $g$  chosen in the direct diagonalization change according to the different single-particle basis sizes  $N_b$ , providing as GS energies respectively  $\mathcal{E} = 1.500$  (a) and  $\mathcal{E} = 2.500$  (b).

To be quantitative, we define the real-space cutoff  $r_c$  as the lower bound of the interval  $(r_c, +\infty)$  within which the wave functions obtained by the renormalized numerical diagonalization and the exact analytic regularization largely overlap. In detail, we define the integral function  $D(r)$  as the deviation of the CI probability density  $r|\Psi_{\text{diag}}(r)|^2$  from its exact counterpart  $r|\Psi_{\text{exact}}(r)|^2$ , which is provided by

¶ This low-lying energy branch of strongly bound molecular dimers is the absolute ground state.



**Table 2.** Real-space cutoff,  $r_c$ , vs number of oscillator orbitals in relative coordinates,  $N_b$ , employed in the direct diagonalization of the two-body ground-state wave function  $\Psi_{\text{diag}}(r)$ . Data of second and third columns correspond to energies  $\mathcal{E} = 1.500$  and  $\mathcal{E} = 2.500$ , being the largest roots of the equation  $D(r_c) = D_{\text{threshold}}$ , with  $D_{\text{threshold}} = 0.02$  and  $0.01$ , respectively. The last column reports the first zero of the  $N_b$ th noninteracting orbital along the radial direction as a reference.

$N_b$	$\mathcal{E} = 1.500$ ( $g < 0$ )	$\mathcal{E} = 2.500$ ( $g > 0$ )	$\mathcal{E} = 2$ ( $g = 0$ )
2	2.58	4.54	2.41
3	2.21	3.57	2.08
4	2.00	3.14	1.91
5	1.86	2.86	1.80
6	1.77	2.67	1.73
10	1.53	2.21	1.55
13	1.41	1.99	1.48

integration between  $r$  and  $\infty$ :

$$D(r) = \int_r^{+\infty} dr' \left| |\Psi_{\text{diag}}(r')|^2 - |\Psi_{\text{exact}}(r')|^2 \right| r'. \quad (12)$$

It is important to note that, since both radial probabilities are separately normalized to one, then  $0 \leq D(r) \leq 1$  and  $D(r) \rightarrow 0$  for  $r \rightarrow 0$ . Furthermore,  $D(r)$  vanishes for  $r \rightarrow \infty$  since both wave functions decay at infinity. From these properties the generic behavior of  $D(r)$  is as follows. First, as  $r$  is reduced from  $\infty$ ,  $D(r)$  remains small as long as  $\Psi_{\text{diag}}(r)$  and  $\Psi_{\text{exact}}(r)$  overlap. Then,  $\Psi_{\text{diag}}(r)$  departs from  $\Psi_{\text{exact}}(r)$  hence  $D(r)$  reaches one or more maxima at certain values of  $r$  and eventually it vanishes again at the origin. Therefore, we define the real-space cutoff  $r_c$  as the largest distance at which

$$D(r_c) = D_{\text{threshold}}, \quad (13)$$

with  $D_{\text{threshold}}$  being conventionally fixed to a few percentages. The values of  $r_c$  as a function of  $N_b$  for the states illustrated in figure 3(a) (attractive;  $D_{\text{threshold}} = 0.02$ ) and figure 3(b) (repulsive;  $D_{\text{threshold}} = 0.01$ ), respectively, are collected in table 2 (note that in the attractive case the convergence is more demanding and we therefore choose a more tolerant threshold value). As expected, the real-space cutoff  $r_c$  decreases with the increasing energy cutoff  $N_b$ . As a reference, in table 2 we also report the first zero of the oscillator orbitals with  $n \leq N_b$  in relative coordinates. All data show similar trends and may be fitted by a power law of the type  $r_c \propto N_b^\beta$ , where  $\beta \approx -0.7$  for  $\mathcal{E} = 1.500$  as well as for  $\mathcal{E} = 2.500$ , and  $\beta \approx -0.6$  for the noninteracting case  $\mathcal{E} = 2$ . These exponents  $\beta$  are not far from the value  $\beta = -0.5$ , hence roughly  $N_b \sim 1/r_c^2$ , i.e., the cutoffs in real and energy spaces are complementary (assuming that the cutoff respectively in momentum space,  $p_c$ , and in real space,  $r_c$ , are related by  $p_c \sim 1/r_c$ ).

### 3. $N$ interacting particles in a trap

So far we have considered the special case of two interacting particles for which the relative motion can be uncoupled from the center-of-mass motion. In this case the results for two spin-1/2 fermions forming a singlet were the same as for two spinless bosons. However, for  $N > 2$  this transformation turns out to be cumbersome for an efficient implementation of the CI algorithm.

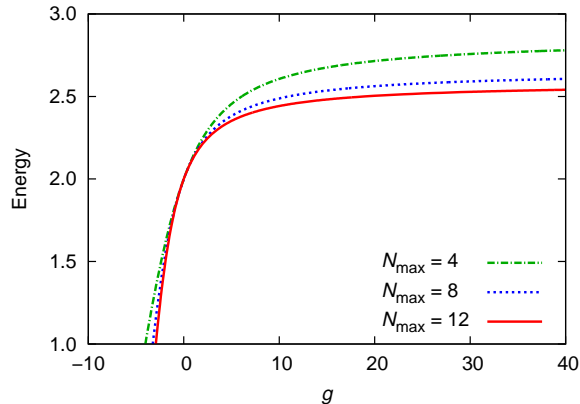


**Figure 4.** (color online) Ground state energy  $\mathcal{E}$  of the two-particle system vs the coupling constant  $g$ . The different lines correspond to different numbers,  $N_{\max}$ , of harmonic oscillator shells employed in the CI diagonalization.

The Hamiltonian of  $N$  particles in a harmonic trap is written in terms of the standard coordinates  $\mathbf{r}_i$  as

$$H_N = \sum_{i=1}^N \left( -\frac{1}{2} \nabla_i^2 + \frac{1}{2} r_i^2 \right) + g \sum_{i<j} \delta(\mathbf{r}_i - \mathbf{r}_j). \quad (14)$$

In typical CI codes the  $N$ -body Hilbert space is spanned over a basis set of Slater determinants for fermions [28–33] or permanents for bosons [57, 58]. The size of the Hilbert space for the  $N$ -body problem is determined by the number of single-particle orbitals from which the Fock states are built. In the 2D harmonic oscillator these single-particle orbitals are grouped in shells according to their single-particle energy. One usually restricts either the noninteracting configurational energy, or simply only includes oscillator shells to a maximum number,  $N_{\max}$ . Here we choose the latter in order to keep the dimensionality well-defined. In the given space and for a given size of the interaction strength  $g$  one then calculates the ground-state energy in the two-body system,  $\mathcal{E} = E_{\text{GS}}^{\text{CI}}(g, N_{\max})$ . The dependence of  $\mathcal{E}$  on the interaction strength parameter is illustrated in figure 4 for a few different basis sizes.

For the  $N = 2$  system, performing the direct CI calculation is alternative to the relative-coordinate approach considered in Section 2. The energy levels up to the third excited state are calculated, and figure 5 shows the convergence for each of the states as the basis size is increased. Here we observe a fast convergence towards the exact values which is well described by a power-law decay in the basis size. The higher-energy states have wave function components involving higher shells and need a larger basis size to converge.

### 3.1. Energy spectrum of three fermions

A semi-analytic solution is available also for three interacting particles in a harmonic trap [52]. Figure 6 compares the exact energies of  $N = 3$  unpolarized fermions (solid lines) with those obtained by the CI method (red [light gray] and blue [dark gray] bullets, respectively, for  $g < 0$  and  $g > 0$ ). The exact energies are obtained following the method reported in reference [52] (there are a few discrepancies with respect to

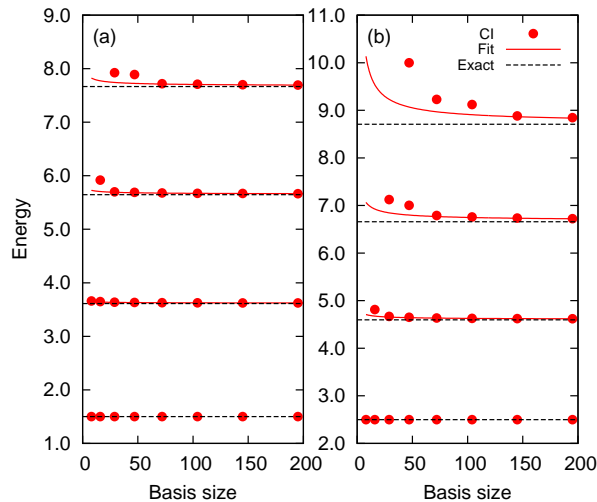


**Figure 5.** (color online) Convergence of the four lowest energy states for two unpolarized fermions versus the many-body basis size in the CI diagonalization. The total angular momentum is  $M = 0$  and calculations are performed for  $N_{\max} = 3$  to 10. The interaction strength  $g$  is determined to give an energy for the two-particle system of  $\mathcal{E} = 1.500$  (a) and  $\mathcal{E} = 2.500$  (b). Solid lines are power-law fits to the data and the dashed lines show the exact values given by (9).

our derivation<sup>+</sup>). Here we focus on the part of the spectrum with angular momentum  $M = 1$ , since it also provides the ground state, and plot the energies as a function of  $\ln(d/a)$ , with  $d = \sqrt{2}$  being the oscillator length in the relative frame. The ground-state energy  $\mathcal{E}$  in the two-particle system is adjusted via the choice of the coupling strength, as described above, and (9) relates it to the scattering length. As the scattering length  $a$  decreases from its infinite positive value at  $\ln(d/a) \rightarrow -\infty$ , the ground-state energy of the  $N = 3$  system departs from the noninteracting value  $E = 4$  and rapidly falls off. First, the CI energies of both ground and excited states match the exact ones very well (up to the fourth digit for the ground state at  $\ln(d/a) = -5.240$  and third digit at  $\ln(d/a) = -1.027$ ). As  $\ln(d/a)$  increases, however, they progressively lose accuracy, as illustrated in table 3. The increasing discrepancy is a consequence of the fact that the energy cutoff induces a real-space cutoff that prevents resolving the wave function when the interparticle separation is too small. This is in particular the case for those low-lying states whose wave functions spatially collapse into strongly bound molecular trimers.

The region  $\ln(d/a) > 0.5$  of figure 6 is considerably more complex, since now two different types of excitations appear: (i) a dense set of ground-state replicas that are tightly bound molecular dimers plus a third spectator particle in an excited level, whose energies have almost vertical slopes, and (ii) a discrete set of curves with moderate slopes that may be regarded as the levels of three fermions with repulsive interactions [52]. Whereas there is no clear-cut distinction between the two types of curves due to the many avoided crossings, the CI method is obviously able to reproduce

<sup>+</sup> Equation (7) in reference [52] should be replaced with our equation (9). Moreover, equation (17) should read  $B_n = (-1)^m [\psi(-\nu_{m,n}) - 2 \ln(d/a)]$ .

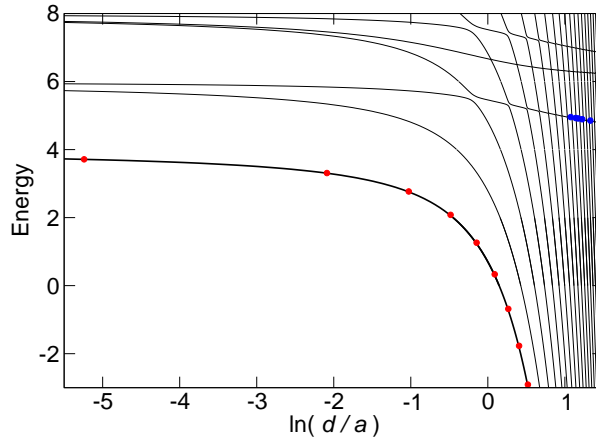


**Figure 6.** (color online) Exact (solid lines) and CI (bullets) energy spectrum of three unpolarized fermions vs scattering length  $a$  for angular momentum  $M = 1$ . Red [light gray] and blue [dark gray] bullets correspond to attractive ( $g < 0$ ) and repulsive ( $g > 0$ ) interactions, respectively. Here  $d = \sqrt{2}$  is the harmonic oscillator length in the relative-motion frame. In the CI calculations we used  $N_{\max} = 10$ .

**Table 3.** Comparison between exact and CI ground-state energies of three unpolarized fermions for attractive interaction, as shown in figure 6 (thick solid line and red [light gray] bullets, respectively). In the CI calculations we used  $N_{\max} = 10$ . The values of the CI coupling constant  $g$  and corresponding scattering length  $a$  are given.

$\ln(d/a)$	exact	$g$	CI
$-\infty$	4	0	4.000
-5.240	3.712	-1	3.713
-2.089	3.305	-2	3.311
-1.027	2.756	-3	2.769
-0.4834	2.061	-4	2.082
-0.1458	1.233	-5	1.263
0.08946	0.2973	-6	0.3338
0.2660	-0.7261	-7	-0.6832
0.4055	-1.817	-8	-1.769
0.5197	-2.963	-9	-2.910

only levels (ii) with significant accuracy. States (i) are clearly beyond the reach of the technique, as the radius of tightly bound dimers is smaller than the minimum spatial resolution associated with the Hilbert space size provided by  $N_{\max}$ .

### 3.2. Energy spectrum of three bosons

A plot similar to figure 6 is shown in figure 7 for three spinless bosons, except that the GS total angular momentum is now  $M = 0$ . In this case the accuracy of the CI calculation is significantly lower than that in figure 6, at least for the lowest-lying branch of strongly bound trimers. The computational bottleneck is the absence of

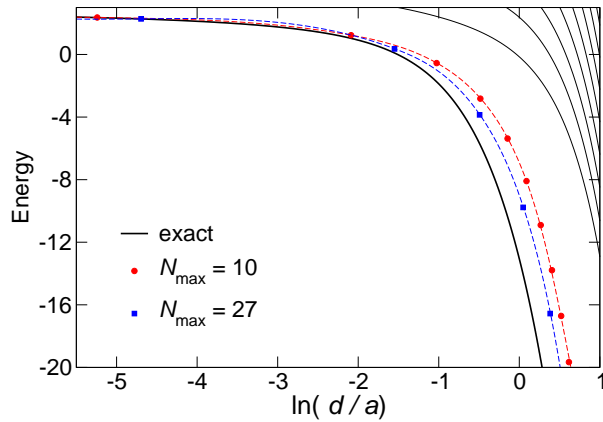


**Figure 7.** (color online) Exact (solid lines) and CI (bullets) energies of three spinless bosons vs scattering length  $a$  for total angular momentum  $M = 0$ . Here  $d = \sqrt{2}$  is the harmonic oscillator length in the relative-motion frame. Respectively,  $N_{\max} = 10$  (circles) and  $N_{\max} = 27$  (squares) oscillator shells were employed in the CI calculation. The dashed lines are cubic smoothing spline interpolations to CI results.

the short-range Pauli repulsion that originates from the exchange between fermions. Even if an increase of the maximum number of oscillator shells  $N_{\max}$  used for the single-particle basis set in the CI diagonalization significantly improves the matching between exact (thick solid line) and CI data (bullets), going from  $N_{\max} = 10$  (circles) to  $N_{\max} = 27$  (squares), the absolute error on the energy is as large as  $\approx 2$  at  $\ln(d/a) \approx -0.5$  and  $\approx 5$  at  $\ln(d/a) \approx 0$ .

### 3.3. Larger systems

For the few-body systems with two and three particles treated so far, exact solutions exist and could be compared to. For larger systems, however, one must solely rely on numerical calculations.

The many-body Hamiltonian given in (14) is diagonalized in a basis of Slater determinants constructed from the lowest  $N_{\max}$  harmonic oscillator shells. In figures 8 and 9, for the example of a system of respectively four and five unpolarized fermions, we show how the energies depend on the size of the Hilbert space used in the CI calculation. Utilizing the discussed concept of renormalization the coupling constant  $g$  together with the basis size are chosen to give a GS energy of the two-particle system of either  $\mathcal{E} = 1.500$  (attractive interactions) or  $\mathcal{E} = 2.500$  (repulsive interactions). We show the two lowest energy states for the four angular momenta  $M = 0, 1, 2$  and  $3$ . For the parameters chosen we find that the energies of low-lying states are well converged for manageable sizes of the Hilbert space.

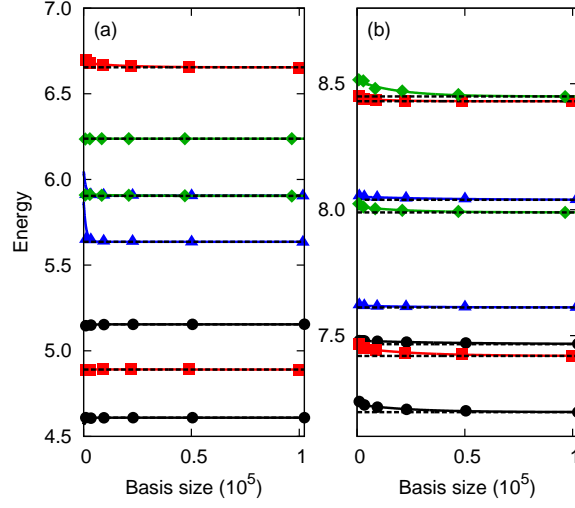


**Figure 8.** (color online) Convergence of the energy spectrum for  $N = 4$  unpolarized fermions vs many-body basis size in the CI diagonalization. The coupling constant  $g$  is determined to give an energy for the two-particle system of  $\mathcal{E} = 1.500$  (a) and  $\mathcal{E} = 2.500$  (b). Here, the two lowest energy states for each of the four total angular momenta  $M = 0, 1, 2$  or  $3$  (circles, triangles, squares, and diamonds, respectively) are shown. Data points are computed for  $N_{\max} = 5$  to  $10$ . Solid lines are exponential fits to the data and dashed lines are their asymptotic values.

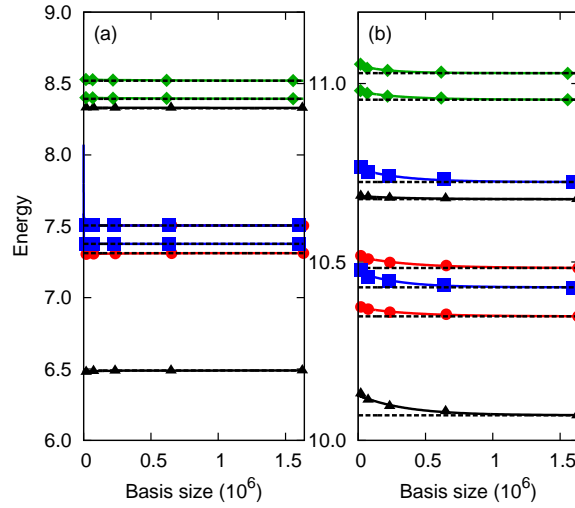


**Figure 9.** (color online) Same as figure 8 but for  $N = 5$  unpolarized fermions.

#### 4. Conclusions

The aim of this paper was to provide a practical ground for CI calculations of  $N$  particles interacting via a contact potential that needs to be properly regularized. To achieve this in a simple and straightforward manner, one renormalizes the strength of the contact potential for two particles in a given subspace of single-particle basis states. The final outcome is that the CI diagonalization over a finite basis set provides physically relevant observables; the energy cutoff only affects the resolution on complementary real space distances, while the low-lying excitation spectrum is unaffected. The procedure discussed here relies on the comparison to both the energy and wave function of two and three particles, obtained in two different ways. The first way is the CI diagonalization with an energy cutoff, while the second one is the exact solution of the Schrödinger equation for the regularized form of the contact pseudopotential. Both ground and excited states are considered in this comparison. The analysis of CI data for a truncated Hilbert space provides a fully consistent physical picture of the results as well as a systematic assessment of the error of the calculation. Finally, the scalability of the method was demonstrated for larger fermionic systems with  $N = 4$  and  $N = 5$  as an example, where no analytical solutions exist and one must rely on numerical calculations. The method converges well for fermionic few-body systems with attractive as well as repulsive interaction, while the bosonic case is found to be more cumbersome. We expect that this procedure may be applied to  $N > 5$ , provided that the radius of studied few-body complexes is larger than the spatial resolution associated with the size of the truncated Hilbert space.

The method discussed here validates previous work, where such *ad hoc* renormalization by simple Hilbert space truncation has been applied, see for example, the discussion of pairing and shell structure in finite-size fermion systems [59], or the recent analysis of few- to many-body transition and the Higgs mode in a paired Fermi gas [60]. The scheme discussed here may be useful for future diagonalization studies in finite-size fermion systems that have now also become experimentally accessible [61–63].

#### Acknowledgments

We thank Jonas Cremon for discussions and for his assistance with part of the numerical work at an early stage of the project, as well as for providing the boson data in Figure 7. We also thank Georg Bruun, Daniela Pfannkuche, Chris Pethick, Ben Mottelson, Vladimir Zelevinsky, and Pavel Kurasov for discussions. This work was supported by EU-FP7 Marie Curie ITN INDEX, by Fondazione Cassa di Risparmio di Modena through the project COLDandFEW, by the CINECA-ISCRA grant IscrC.TUN1DFEW, as well as by NordForsk, the Swedish Foundation for Strategic Research, the Swedish Research Council, and NanoLund at Lund University.

#### References

- [1] F. Dalfovo, S. Giorgini, L. P. Pitaevskii, and S. Stringari. Theory of Bose-Einstein condensation in trapped gases. *Rev. Mod. Phys.*, 71:463–512, 1999.
- [2] A. J. Leggett. Bose-Einstein condensation in the alkali gases: Some fundamental concepts. *Rev. Mod. Phys.*, 73:307–356, 2001.
- [3] C. J. Pethick and H. Smith. *Bose-Einstein Condensation in Dilute Gases*. Cambridge University Press, Cambridge (UK), 2002.

- [4] L. Pitaevskii and S. Stringari. *Bose-Einstein Condensation*. Oxford University Press, Oxford, 2003.
- [5] A. J. Leggett. *Quantum Liquids*. Oxford University Press, Oxford, 1st edition, 2006.
- [6] I. Bloch, J. Dalibard, and W. Zwerger. Many-body physics with ultracold gases. *Rev. Mod. Phys.*, 80:885–964, 2008.
- [7] S. Giorgini, L. P. Pitaevskii, and S. Stringari. Theory of ultracold atomic Fermi gases. *Rev. Mod. Phys.*, 80:1215–1274, 2008.
- [8] K. Huang. *Statistical Mechanics*. Wiley, New York, 1963.
- [9] V. M. Galitskii. The energy spectrum of a non-ideal Fermi gas. *Soviet Phys. JETP*, 34:104–112, 1958.
- [10] L. P. Gor'kov and T. K. Melik-Barkhudarov. Contribution to the theory of superfluidity in an imperfect Fermi gas. *Soviet Phys. JETP*, 13:1018–1022, 1961.
- [11] A. J. Leggett. Diatomic molecules and Cooper pairs. In A. Pekalski and A. Przystawa, editors, *Modern Trends in the Theory of Condensed Matter*, volume 115 of *Lecture Notes in Physics*, chapter 2, pages 13–27. Springer-Verlag, Berlin, 1980.
- [12] S. Adhikari and A. Ghosh. Renormalization in non-relativistic quantum mechanics. *J. Phys. A: Math. Gen.*, 30:6553, 1997.
- [13] A. Ghosh, S. Adhikari, and B. Talukdar. Dimensional versus cut-off renormalization and the nucleon-nucleon interaction. *Phys. Rev. C*, 58:1913–1920, 1998.
- [14] H. E. Camblong and C. R. Ordóñez. Renormalized path integral for the two-dimensional  $\delta$ -function interaction. *Phys. Rev. A*, 65:052123, 2002.
- [15] L. Pricoupenko. Pseudopotential in resonant regimes. *Phys. Rev. A*, 73:012701, 2006.
- [16] A. Sütó. Exact eigenstates for contact interactions. *J. Stat. Phys.*, 109:1051–1072, 2002.
- [17] T. Busch, B.-G. Englert, K. Rzążewski, and M. Wilkens. Two cold atoms in a trap. *Found. Phys.*, 28:549–559, 1998.
- [18] A. Cabo, J. L. Lucio, and H. Mercado. On scale invariance and anomalies in quantum mechanics. *Am. J. Phys.*, 66:240–246, 1998.
- [19] B. D. Esry and C. H. Greene. Validity of the shape-independent approximation for Bose-Einstein condensates. *Phys. Rev. A*, 60:1451–1462, 1999.
- [20] Y. Castin. Bose-Einstein condensates in atomic gases: Simple theoretical results. In R. Kaiser, C. Westbrook, and F. David, editors, *Coherent Atomic Matter Waves*, Lectures Notes of Les Houches Summer School, pages 1–136. EDP Sciences and Springer-Verlag, Berlin, 2001.
- [21] L. Pricoupenko. Isotropic contact forces in arbitrary representation: Heterogeneous few-body problems and low dimensions. *Phys. Rev. A*, 83:062711, 2011.
- [22] R. A. Doganov, S. Klaiman, O. E. Alon, A. I. Streltsov, and L. S. Cederbaum. Two trapped particles interacting by a finite-range two-body potential in two spatial dimensions. *Phys. Rev. A*, 87:033631, 2013.
- [23] D. Blume, J. von Stecher, and C. H. Greene. Universal properties of a trapped two-component Fermi gas at unitarity. *Phys. Rev. Lett.*, 99:233201, 2007.
- [24] J. von Stecher and C. H. Greene. Spectrum and dynamics of the BCS-BEC crossover from a few-body perspective. *Phys. Rev. Lett.*, 99:090402, 2007.
- [25] J. von Stecher, C. H. Greene, and D. Blume. BEC-BCS crossover of a trapped two-component Fermi gas with unequal masses. *Phys. Rev. A*, 76:053613, 2007.
- [26] J. von Stecher, C. H. Greene, and D. Blume. Energetics and structural properties of trapped two-component Fermi gases. *Phys. Rev. A*, 77:043619, 2008.
- [27] J. Christensson, C. Forssén, S. Åberg, and S. M. Reimann. Effective-interaction approach to the many-boson problem. *Phys. Rev. A*, 79:012707, 2009.
- [28] R. McWeeny. *Methods of Molecular Quantum Mechanics*. Academic Press, London, 1992.
- [29] T. Helgaker, P. Jørgensen, and J. Olsen. *Molecular Electronic-Structure Theory*. Wiley, Chichester, England, 2000.
- [30] F. Jensen. *Introduction to Computational Chemistry*. Wiley, Chichester, England, 2007.
- [31] M. Brasken, M. Lindberg, D. Sundholm, and J. Olsen. Full configuration interaction calculations of electron-hole correlation effects in strain-induced quantum dots. *Phys. Rev. B*, 61:7652–7655, 2000.
- [32] S. M. Reimann and M. Manninen. Electronic structure of quantum dots. *Rev. Mod. Phys.*, 74:1283–1342, 2002.
- [33] M. Rontani, C. Cavazzoni, D. Bellucci, and G. Goldoni. Full configuration interaction approach to the few-electron problem in artificial atoms. *J. Chem. Phys.*, 124:124102, 2006.
- [34] A. Fetter. Rotating trapped Bose-Einstein condensates. *Rev. Mod. Phys.*, 81:647–691, 2009.
- [35] Y. Castin. Simple theoretical tools for low dimension Bose gases. *J. Phys. IV*, 116:89–132, 2004.



- [36] J. E. Drut and A. N. Nicholson. Lattice methods for strongly interacting many-body systems. *J. Phys. G: Nucl. Part. Phys.*, 40:043101, 2013.
- [37] E. Braaten and A. Nieto. Quantum corrections to the ground state of a trapped Bose-Einstein condensate. *Phys. Rev. B*, 56:14745–14765, 1997.
- [38] A. Bulgac, J. E. Drut, and P. Magierski. Spin 1/2 fermions in the unitary regime: A superfluid of a new type. *Phys. Rev. Lett.*, 96:090404, 2006.
- [39] J. von Stecher and C. H. Greene. Renormalized mean-field theory for a two-component Fermi gas with  $s$ -wave interactions. *Phys. Rev. A*, 75:022716, 2007.
- [40] I. Stetcu, B. R. Barrett, and U. van Kolck. No-core shell model in an effective-field-theory framework. *Phys. Lett. B*, 653:358–362, 2007.
- [41] I. Stetcu, B. R. Barrett, U. van Kolck, and J. P. Vary. Effective theory for trapped few-fermion systems. *Phys. Rev. A*, 76:063613, 2007.
- [42] Y. Alhassid, G. F. Bertsch, and L. Fang. New effective interaction for the trapped Fermi gas. *Phys. Rev. Lett.*, 100:230401, 2008.
- [43] N. T. Zinner, K. Mølmer, C. Özen, D. J. Dean, and K. Langanke. Shell-model Monte Carlo simulations of the BCS-BEC crossover in few-fermion systems. *Phys. Rev. A*, 80:013613, 2009.
- [44] C. N. Gilbreth and Y. Alhassid. Separable effective interaction for the trapped Fermi gas: The BEC-BCS crossover. *Phys. Rev. A*, 85:033621, 2012.
- [45] S. Tölle, H.-W. Hammer, and B. C. Metsch. Convergence properties of the effective theory for trapped bosons. *J. Phys. G: Nucl. Part. Phys.*, 40:055004, 2013.
- [46] C. N. Gilbreth and Y. Alhassid. Pair condensation in a finite trapped Fermi gas. *Phys. Rev. A*, 88:063643, 2013.
- [47] A. Bulgac and Y. Yu. Renormalization of the Hartree-Fock-Bogoliubov equations in the case of a zero range pairing interaction. *Phys. Rev. Lett.*, 88:042504, 2002.
- [48] L. Pricoupenko. Variational approach for the two-dimensional trapped Bose-Einstein condensate. *Phys. Rev. A*, 70:013601, 2004.
- [49] C. W. Johnson. Many-body fits of phase-equivalent effective interactions. *Phys. Rev. C*, 82:031303(R), 2010.
- [50] I. Boettcher, J. M. Pawłowski, and S. Diehl. Ultracold atoms and the functional renormalization group. *Nucl. Phys. B (Proc. Suppl.)*, 228:63–135, 2012.
- [51] Y. Yan and D. Blume. Incorporating exact two-body propagators for zero-range interactions into  $N$ -body Monte Carlo simulations. *Phys. Rev. A*, 91:043607, 2015.
- [52] X.-J. Liu, H. Hu, and P. D. Drummond. Three attractively interacting fermions in a harmonic trap: Exact solution, ferromagnetism, and high-temperature thermodynamics. *Phys. Rev. B*, 82:054524, 2010.
- [53] M. Olshanii and L. Pricoupenko. Rigorous approach to the problem of ultraviolet divergencies in dilute Bose gases. *Phys. Rev. Lett.*, 88:010402, 2002.
- [54] D. S. Petrov and G. V. Shlyapnikov. Interatomic collisions in a tightly confined Bose gas. *Phys. Rev. A*, 64:012706, 2001.
- [55] S. A. Coon, M. I. Avetian, M. K. G. Kruse, U. van Kolck, P. Maris, and J. P. Vary. Convergence properties of ab initio calculations of light nuclei in a harmonic oscillator basis. *Phys. Rev. C*, 86:054002, 2012.
- [56] S. König, S. K. Bogner, R. J. Furnstahl, S. N. More, and T. Papenbrock. Ultraviolet extrapolations in finite oscillator bases. *Phys. Rev. C*, 90:064007, 2014.
- [57] D. Sundholm and T. Vänskä. A configuration interaction approach to bosonic systems. *J. Phys. B: At. Mol. Opt. Phys.*, 37:2933–2942, 2004.
- [58] A. Szabados, P. Jeszenszki, and P. R. Surján. Efficient iterative diagonalization of the Bose-Hubbard model for ultracold bosons in a periodic optical trap. *Chem. Phys.*, 401:208–216, 2012.
- [59] M. Rontani, J. R. Armstrong, Y. Yu, S. Åberg, and S. M. Reimann. Cold fermionic atoms in two-dimensional traps: Pairing versus Hund's rule. *Phys. Rev. Lett.*, 102:060401, 2009.
- [60] J. Bjerlin, S. M. Reimann, and G. M. Bruun. Few-body precursor of the Higgs mode in a Fermi gas. *Phys. Rev. Lett.*, 116:155302, 2016.
- [61] F. Serwane, G. Zürn, T. Lompe, T. B. Ottenstein, A. N. Wenz, and S. Jochim. Deterministic preparation of a tunable few-fermion system. *Science*, 332:336–338, 2011.
- [62] G. Zürn, A. N. Wenz, S. Murmann, A. Bergschneider, T. Lompe, and S. Jochim. Pairing in few-fermion systems with attractive interactions. *Phys. Rev. Lett.*, 111:175302, 2013.
- [63] A. N. Wenz, G. Zürn, S. Murmann, I. Brouzos, T. Lompe, and S. Jochim. From few to many: Observing the formation of a Fermi sea one atom at a time. *Science*, 342:457–460, 2013.